

Tunneling and resonant tunneling of fluxons in a long Josephson junction

Alexander Shnirman and Eshel Ben-Jacob

School of Physics and Astronomy, Raymond and Beverly Sackler Faculty of Exact Sciences, Tel-Aviv University, Ramat-Aviv, 69978 Tel-Aviv, Israel

Boris Malomed

School of Mathematical Sciences, Raymond and Beverly Sackler Faculty of Exact Sciences, Tel-Aviv University, Ramat-Aviv, 69978 Tel-Aviv, Israel

(Received 23 May 1996; revised manuscript received 4 November 1996)

We study fluxon tunneling both across one microshort-type barrier and resonant tunneling across two barriers. We have derived an effective Hamiltonian (using the inverse scattering transform) to study the effect of plasmons on the tunneling. Using a specially derived perturbation scheme, we found two effects: (1) Emission of plasmons and, hence, suppression of quantum effects. Due to the gap in the plasmon spectrum, this is an exponentially small effect. (2) Virtual processes involving plasmons' emission and absorption cause an enhancement of the tunneling probability. The magnitude of this enhancement is not exponentially small. We conclude that macroscopic quantum tunneling of fluxons can be observed. We further predict that fluxons' resonant tunneling across two barriers can also be observed. This phenomenon provides an ideal test for the quantum behavior of the fluxons. [S0163-1829(97)02942-1]

I. INTRODUCTION

The fundamental question whether particlelike collective excitations, like domain walls, vortices or fluxons, can exhibit quantum behavior has attracted much attention in the last years.^{1,2} When the mass of an excitation becomes small enough, quantum effects are, in principle, expected. These effects usually fall into two major classes—interference and tunneling. Observations of the interference effects (weak localization, universal fluctuations, etc.) are usually suppressed by various dephasing mechanisms, emerging from the coupling of the collective excitation to some other degrees of freedom. The effect of the latter on quantum tunneling is more involved. On one hand, the coupling can cause dissipation and, hence, reduction of the tunneling probability.³ On the other hand, the coupling enlarges the variety of possible zero-mode fluctuations, thus enabling the particle to find a “better pass” in the classically forbidden regions.⁴

In this paper we consider the tunneling of a fluxon through δ -function-like barriers in a long Josephson junction. By δ -function-like we mean that the width of the barrier is much shorter than the Josephson penetration length λ_J . To create a potential barrier for the fluxon, a microshort has to be included. Namely, the Josephson energy at the microshort regime has to be larger than along the rest of the junction. The phenomenon of soliton's tunneling has been studied in charge-density-wave systems.⁵ In the case of a weak impurity (energy of the impurity barrier is smaller than the soliton's rest energy) the soliton was treated as a free particle interacting only with a stiff localized potential barrier. Here we take a different approach in which we take into account the soliton's shape deformations due to coupling to plasmons. We neglect other dephasing mechanisms except for the coupling to plasmons. The latter is unique because the plasmons are the excitations of the same field as the fluxon itself. All other mechanisms (quasiparticle tunneling, disorder

etc.) are quite similar to the ones occurring for an electron in a dephasing medium.⁶ The effect of Ohmic dissipation on the fluxon's tunneling was recently considered in Ref. 7. At mK temperatures, where we expect to observe quantum phenomena, the Ohmic dissipation is mostly due to subgap conductance,⁸ which results, for example, from paramagnetic impurities. Here we neglect this source of Ohmic dissipation, i.e., we assume high-quality junctions.

First, we consider a one-barrier situation. We derive an effective Hamiltonian using the inverse scattering transform (IST).⁹ The advantage of this technique is that it produces an asymptotically free Hamiltonian (the coupling between the fluxon and the plasmons is nonzero only in the impurity's vicinity). Next we develop a special perturbation scheme, which enables us to take into account the tunneling process in the zeroth order approximation. Our calculations show that although the fluxons are macroscopic objects with internal degrees of freedom they can exhibit measurable quantum tunneling.

Experimentally it is hard to distinguish between quantum tunneling and effects of excess noise which lead to classical activation above the barrier. We propose the resonant tunneling to be a better test of the quantum behavior. Classically the probability for activation above two closely located barriers is the product of the activation probabilities across each barrier separately. Hence it is extremely small. Quantum mechanically the tunneling probability across two barriers can be close to one provided the particle has an energy compatible with the energy level of a quantum state between the two barriers. It is also true if dephasing mechanisms do not destroy the quantum coherence of the motion between the barriers. We have calculated the plasmons' effect on resonant tunneling. Our findings show that fluxons can perform resonant tunneling in spite of coupling to plasmons. Hence we propose to look for resonant tunneling as a clear cut test of fluxons' quantum behavior.

II. THE MODEL

An ideal long Josephson junction is described by the following Lagrangian:^{10,11}

$$L_0 = \frac{\hbar \bar{c}}{\beta^2} \int_{-\infty}^{+\infty} \left[\frac{1}{2\bar{c}^2} \dot{\theta}^2 - \frac{1}{2} \theta_x^2 - \frac{1}{\Lambda_J^2} (1 - \cos \theta) \right] dx, \quad (1)$$

where θ is the gauge-invariant phase difference across the junction, \bar{c} is the Swihart velocity, and the parameter β is defined as follows:

$$\beta^2 \equiv 16\pi \frac{e^2}{\hbar c} \frac{\sqrt{(2\lambda_L + d)d}}{W}. \quad (2)$$

Here λ_L is the London penetration depth, d is the thickness of the insulating layer, and W is the width of the junction.

This well-known sine-Gordon model exhibits two kinds of excitations. The first one is a topological soliton, called a fluxon, which may be thought of as a relativistic massive particle.^{11,12} All other excitations are nontopological. They include linear electromagnetic waves (plasmons) and their bound states (breathers).^{9,13} The breathers can be equivalently presented as fluxon-antifluxon bound states or as bound states of plasmons. This will not make a difference in our further considerations. Due to the complete integrability of the sine-Gordon model, all excitations are decoupled. Hence, we may consider the fluxon as a free particle. This situation changes when interference phenomena are considered.¹⁴ The situation also changes when an impurity is inserted into the junction. In this case one should add to Eq. (1) the following term:¹¹

$$L_{\text{imp}} = - \frac{\hbar \bar{c}}{\beta^2} \int_{-\infty}^{+\infty} \frac{\epsilon \delta(x-a)}{\Lambda_J} (1 - \cos \theta) dx. \quad (3)$$

Here a is the impurity's position and ϵ is its strength. The additional term corresponds to a short (compared to Λ_J) region Δx , where the density of the Josephson energy E_J is changed by ΔE_J . Thus, in the δ -function approximation, we estimate ϵ as follows:

$$\epsilon = \frac{\Delta x \Delta E_J}{\Lambda_J E_J}. \quad (4)$$

Positive ϵ corresponds to a microshort-type impurity, which means that the Josephson energy at the impurity is larger than in the rest of the junction. It is clear that this type of impurity will create a potential barrier for a fluxon, since the interaction energy has a maximum when the fluxon's center coincides with the impurity.¹¹ Moreover, the impurity will cause a coupling between the excitations of the system. Particularly, the coupling between a fluxon and plasmons may be easily understood if one notes that, while approaching the impurity, the fluxon will be changing its shape, which is equivalent to excitation of plasmons.

A very special role is played by the parameter β . This constant determines the overall coefficient in front of the Lagrangian, thus it does not affect the equations of motion. Nevertheless, it sets the energy scale in the particular system. One can show¹⁵ that the ratio of the fluxon's mass M to the plasmon's mass m is given by

$$\frac{M}{m} = \frac{8}{\beta^2}, \quad (5)$$

for small enough values of β^2 . Inserting Eq. (1) into a path integral, one can see¹⁰ that β^2 effectively renormalizes the Planck's constant \hbar . So the larger the β^2 , the smaller the energy scale of the system, and, therefore, the more quantum the system is. The β^2 constant may also be interpreted in the following way:

$$\beta^2 = \sqrt{\frac{E_C}{E_L}}, \quad (6)$$

where E_C and E_L are the characteristic charging and inductive energies of the junction, respectively.^{10,16} Now with the micro-fabrication technique one can build junctions with values of β^2 such that quantum phenomena are expected to be observed.^{27,28}

We proceed to derive an effective Hamiltonian, which will describe the fluxon as a massive particle scattered by the potential barrier created by the impurity. The fictitious particle should be coupled to the plasmons in a λ_J vicinity of the impurity and should be free outside this regime. To this end, we develop a perturbation scheme based on the inverse scattering transform (IST),⁹ the only technique which provides a completely decoupled Hamiltonian outside the impurities' region. Earlier such schemes were developed to study the solitons' classical dynamics.^{11,17-19} Those schemes are based on the smallness of the plasmons' amplitude. We have developed a different approach. First, the impurity contribution to the Hamiltonian ($-L_{\text{imp}}$) is expressed in terms of the IST dynamical variables. Then, we expand the Hamiltonian in powers of β . For small β , we restrict the expansion to the terms linear in β and derive the following Hamiltonian (see Appendix A):

$$H = \frac{P^2}{2M} + \frac{\epsilon}{\beta^2} V_0 + H_{\text{free}} + H_{\text{int}}, \quad (7)$$

where

$$H_{\text{free}} = \int_{-\infty}^{+\infty} \omega_k d_k^* d_k dk, \quad (8)$$

$$H_{\text{int}} = \frac{\epsilon}{4\sqrt{\pi}\beta} \left[iV_1 \int_{-\infty}^{+\infty} \frac{d_k e^{ika} - d_k^* e^{-ika}}{\omega_k^{3/2}} dk + V_2 \int_{-\infty}^{+\infty} \frac{d_k e^{ika} + d_k^* e^{-ika}}{\omega_k^{3/2}} k dk + O\left(\frac{v}{c}, \beta^2\right) \right], \quad (9)$$

$$V_0 = \frac{2}{\cosh^2(X-a)}, \quad (10)$$

$$V_1 = \frac{4 \tanh^2(X-a)}{\cosh(X-a)}, \quad (11)$$

$$V_2 = \frac{2 \tanh(X-a)}{\cosh(X-a)}. \quad (12)$$

Here, X and P are the fluxon's collective coordinate and momentum, while d_k and d_k^* are the plasmons' conjugate

variables (prototypes of the quantum creation and annihilation operators). The plasmon dispersion relation is $\omega_k^2 = 1 + k^2$. We consider the nonrelativistic limit (small fluxon velocity): H_{int} includes only terms which are zero order in v/\bar{c} .

The Hamiltonian (7) can be viewed as the Hamiltonian of a particle with mass M , moving in the presence of a potential V_0 , and coupled to a bath of free plasmons. The H_{int} term describes the coupling between the fluxon and the plasmons, which vanishes at plus and minus infinity. The Hamiltonian is expressed in the usual dimensionless units: the length is measured in units of Λ_J , the frequency is measured in units of $\omega_J \equiv \bar{c}/\Lambda_J$, and the action is measured in units of \hbar . In this notation the mass of the plasmon is one, the energy unit is the plasmons rest energy $\hbar\omega_J$, and the mass of the fluxon is $8/\beta^2$.

The Hamiltonian (7) corresponds to a single-impurity situation. To construct a many-impurity Hamiltonian one should add the corresponding V_0 and H_{int} terms for each of the impurities, accounting for their positions a_n and their strengths ϵ_n .

Next we quantize the Hamiltonian (7) using the canonical prescription. This quantization effectively means treating the field θ as a quantum one. As was shown by Widom,²⁰ the canonical commutation relations between $\theta(x,t)$ and $\rho(x,t) \propto \dot{\theta}(x,t)$ follow directly from the commutation relations between the operators of the electric field E and magnetic field B . Thus our quantization procedure is nothing else but the quantization of the electromagnetic field in the junction. A further insight of the quantization procedure is presented by Schön and Zaikin.⁸

III. ONE-BARRIER TUNNELING

Tunneling is a nonperturbative phenomenon. Thus, we should build a perturbation scheme including tunneling at the zeroth order, and treating perturbatively only the fluxon-plasmon coupling terms (9). Following Dyson's perturbation theory²¹ we have developed a perturbation scheme in which H_0 includes the first three terms of Eq. (7) (See Appendix B for details):

$$H_0 = \frac{P^2}{2M} + \frac{\epsilon}{\beta^2} V_0 + H_{\text{free}}. \quad (13)$$

Let us consider the tunneling through an impurity placed at $x=0$. We use Eqs. (B5) and (B6) to determine the forward and backward elastic scattering probabilities. Due to the symmetry of the potential barrier V_0 , the following relation holds:

$$r_0 t_0^* = -r_0^* t_0 \equiv iD, \quad (14)$$

where $D(E)$ is a real function of energy. As we will see later, the sign of D is of a crucial importance. From Eq. (14) it follows that D can change its sign only at the energies for which $t_0=0$ or $|t_0|=1$. For the one-barrier case, this may happen only above the barrier, so D does not change sign for energies below the barrier. One can check that in this case D is always negative (irrespective of the particular form of V_0). We calculate the matrix elements A and B at the second order of perturbation theory (See Appendix B) to obtain

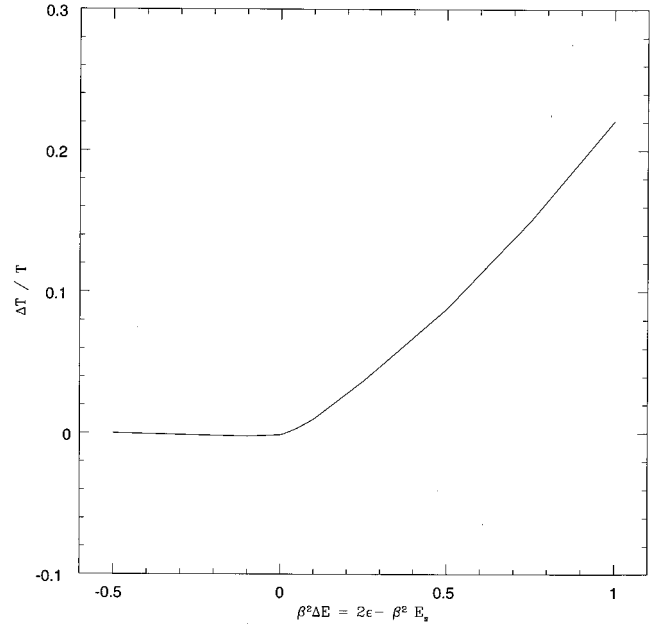


FIG. 1. The relative change of the tunneling probability as a function of the difference between the barrier's top energy and the soliton's energy.

$$|t(E)|^2 = [1 + 2 \operatorname{Re}(A)] |t_0|^2 - 2 \operatorname{Im}(B)D, \quad (15)$$

and

$$|r(E)|^2 = [1 + 2 \operatorname{Re}(A)] |r_0|^2 + 2 \operatorname{Im}(B)D. \quad (16)$$

One can distinguish two effects in Eqs. (15) and (16). The first one is the decrease due to inelastic processes of the total probability of the elastic scattering, which is now $[1 + 2 \operatorname{Re}(A)]$ instead of 1 [note that $\operatorname{Re}(A)$ should be negative]. The inelastic processes include at least one real plasmon emitted. Thus the probability of such processes is exponentially small due to the gap in the plasmon spectrum. The matrix element A contains a factor $\exp(-\omega_j\tau)$, where τ is the Buttiker-Landauer tunneling time.²³

The second effect is a redistribution between the elastic forward and backward scattering probabilities. The redistribution term $2 \operatorname{Im}(B)D$ is not related to the real plasmons, but to the virtual ones. For this reason the term is not exponentially small. We have evaluated the redistribution term numerically, using the exact zeroth-order fluxon wave functions, and found that, at the energies lying deep below the barrier, the tunneling probability is enhanced. The relative increment (the ratio of the tunneling probability increment to the total tunneling probability) increases with decrease of the fluxon's energy. The tunneling probability is slightly reduced in a very narrow interval of energies near the top of the barrier (see Fig. 1). The change in the tunneling probability due to the coupling with plasmons can be expressed as a change ΔV_{Born} in the potential in the absence of plasmons. Using the first-order Born approximation (Appendix B) we obtain

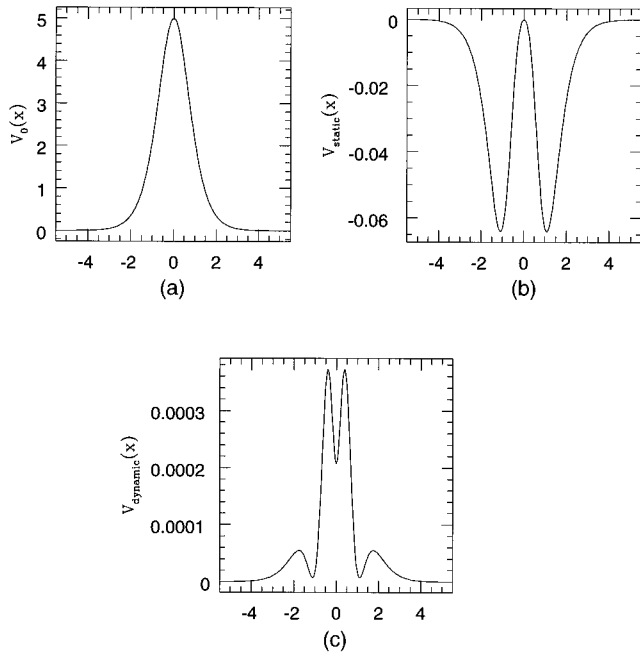


FIG. 2. (a) The unperturbed potential barrier; (b) the narrowing (static) correction; (c) the dynamic correction, which makes the barrier taller.

$$\Delta V_{\text{Born}} = -\frac{\epsilon^2}{32\beta^2} [V_1^2(x) + V_2^2(x)] + \frac{\epsilon^2}{256\pi} \left(\frac{4}{3} V_1'^2(x) + \frac{2}{3} V_2'^2(x) \right). \quad (17)$$

One can see that the first term of Eq. (17), which vanishes at $x=0$, narrows the total potential barrier, while the second term, which does not vanish at $x=0$, makes the barrier taller (see Fig. 2). Since the first term is much larger than the second one (β is small), the main effect is the barrier's narrowing and, therefore, enhancement of the tunneling.

This result means that not only fluxons' quantum tunneling can be observed in the presence of coupling with plasmons but the effect can even be enhanced. This phenomenon results from the energy gap in the plasmons' spectrum and the fact that the coupling is limited to the vicinity of the potential barrier, as we show in the next section.

IV. PATH-INTEGRAL APPROACH

To go beyond the perturbation theory we apply a Caldeira-Legget-type approach.^{3,24} We integrate out the plasmon degrees of freedom in the complex time to obtain the usual addition to the effective action in the path integral:

$$\Delta S = \Delta S_1 + \Delta S_2, \quad (18)$$

where

$$\Delta S_i = -\frac{\epsilon^2}{32\pi\beta^2} \int \int d\tau d\tau' G_i(|\tau - \tau'|) V_i(X(\tau)) \times V_i(X(\tau')), \quad (19)$$

$$G_1 = \int dk \frac{1}{\omega_k} e^{-\omega_k|\tau - \tau'|}, \quad (20)$$

$$G_2 = \int dk \frac{k^2}{\omega_k} e^{-\omega_k|\tau - \tau'|}. \quad (21)$$

The situation here resembles the scanning-tunneling microscopy (STM) "image potential."²⁴ Using the fact that for $\epsilon < 1$ the tunneling time is much longer than the maximum plasmon period $2\pi/\omega_0$, we apply the adiabatic approximation to Eq. (19) and we arrive at the following static potential correction:

$$\Delta V = -\frac{\epsilon^2}{32\beta^2} [V_1^2(x) + V_2^2(x)], \quad (22)$$

which coincides with the first term of Eq. (17). We did not calculate the dynamical corrections to Eq. (22), which, according to Ref. 24, suppress the tunneling. Nevertheless, it is quite clear that dynamical corrections may become important at the energies close to the barrier's top, since the static corrections vanish there. Thus, we again obtain the result specified in the previous section: there is a static narrowing correction to the potential barrier, accompanied by a small dynamical correction, which effectively makes the barrier taller.

Note that the static correction (22) has a classical interpretation. A fluxon forced externally to be located at a position x will act on the plasmons to change their equilibrium positions in order to minimize the energy corresponding to the two last terms of the Hamiltonian (7). The energy gain of this relaxation is exactly equal to the static potential correction (22). Moreover, we guess that every effective potential correction for the elastic processes has its classical analog. Indeed, the dynamical corrections may be understood as the induced kinetic energy of the plasmons during the fluxon's passage through the barrier. Since this energy is finally returned to the fluxon, it may be interpreted as a correction to the potential energy of the barrier.

Note that there are two main differences between our system and that of Caldeira and Legget's one. First, the Caldeira-Legget thermal bath has no gap in the energy spectrum. Therefore, the main process during tunneling is the real emittance of radiation, i.e., dissipation of energy. In our system the elastic processes are the most relevant ones due to the plasmon's energy gap. Second, the coupling between the particle and the bath is homogeneous in the Caldeira-Legget situation. Therefore, the static potential corrections just renormalize the total energy by a constant. In our system the coupling is nonzero at the barrier's vicinity only, so the static correction becomes dominant.

V. RESONANT TUNNELING

As we have mentioned in the introduction a possible observation of resonant tunneling of fluxons would be the most persuasive evidence of their quantum behavior. For this reason we study here whether the resonant tunneling phenomenon survives in the presence of coupling to plasmons.

We insert two identical δ -like impurities ($\epsilon_1 = \epsilon_2 \equiv \epsilon$) at the points $x=a$ and $x=-a$, thus producing a symmetric

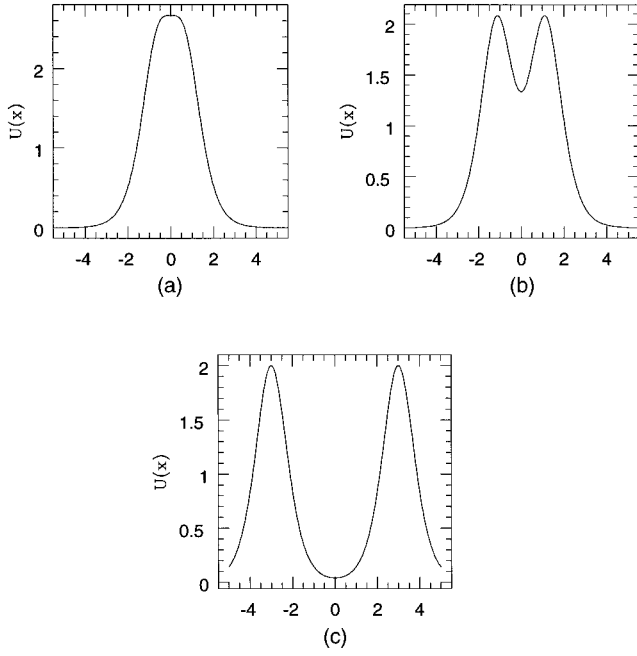


FIG. 3. Double impurity potential: (a) at $a = \cosh^{-1}(\sqrt{3/2})$; (b) at $a = \cosh^{-1}(\sqrt{3})$; (c) at $a = 3.0$.

setup. Neglecting in the zeroth approximation the fluxon-plasmons coupling, we obtain the following potential acting on a fluxon:

$$U(X) = \frac{\epsilon}{\beta^2} [V_0(X-a) + V_0(X+a)]. \quad (23)$$

We see that three very different physical regimes emerge as we vary the distance between the impurities (see Fig. 3). First, for small a , the total potential is a simple barrier with only one maximum. Then, above $a = \cosh^{-1}(\sqrt{3/2})$, the double-barrier structure appears with a shallow potential well in the center. This well may be characterized by the curvature at its bottom ($x=0$), which determines the frequency of the quasilevels in the well, $\Omega^2 = 2U''(0)/M$. We find that Ω increases from zero at $a = \cosh^{-1}(\sqrt{3/2})$ up to its maximum value $\Omega_{\max} = \sqrt{\epsilon/3}$ at $a = \cosh^{-1}(\sqrt{3})$. Above this value of a Ω decreases again as the two barriers become separated. Thus we find that the largest level separation takes place at $a = \cosh^{-1}(\sqrt{3})$. The number of levels in the well, N , is approximately $\sqrt{\epsilon/\beta^2}$. For typical junctions' parameters N can be much larger than one. Nevertheless, we expect that with the modern technology one can construct a junction for which there are only a few levels in the well.

We examine now the effect of plasmons on the resonant tunneling at $a = \cosh^{-1}(\sqrt{3})$. First we note that the coupling between the fluxon and plasmons at the outer slopes of the combined potential barrier has the same effect as in the case of single impurity. It slightly reduces the total width of the barrier, thus, slightly increasing the total (nonresonant) transmission probability and, simultaneously, slightly widening the quasilevels in the well. A much stronger coupling appears inside the well (at the inner slopes of the humps) due to the large values of the fluxon wave functions there. This kind of problem is usually efficiently treated by the tunnel-Hamiltonian method, i.e., by dividing the system into three

parts: left and right leads and the potential well itself.²⁵ The coupling between the parts is through the tunneling hybridization (one-barrier tunneling). It is easy to see that every quasilevel, n , in the well has the following contribution to the well's Hamiltonian:

$$\begin{aligned} H_n &= \int dk \alpha_{nk} (d_k - d_k^\dagger) c_n^\dagger c_n \\ &= \frac{\epsilon i}{(4\sqrt{\pi}\beta)} c_n^\dagger c_n \int dk \left(M_{1n} \frac{\sin ka}{\omega_k^{3/2}} + M_{2n} \frac{\cos ka}{\omega_k^{3/2}} k \right) \\ &\quad \times (d_k - d_k^\dagger), \end{aligned} \quad (24)$$

where

$$M_{1,2n} \equiv \int dx V_{1,2}(x-a) |\Psi_n(x)|^2, \quad (25)$$

and c_n^\dagger is an operator creating a fluxon at the n 's level. Then the total well Hamiltonian may be exactly diagonalized by a canonical transformation.²¹ In the case of many levels in the well, the diagonalization is valid only for one-particle problems. The result is that every level acquires a polaron shift:

$$\Delta E_n = \int dk \frac{|\alpha_{nk}|^2}{\omega_k}. \quad (26)$$

Besides this, the replica resonances may appear²⁵ for every particular level. For the few-levels case, the replica do not belong to the well's interval of energies. Thus we conclude that, at least for a situation with a few levels, the only plasmon effect is the polaron shift of the levels. The plasmons do not destroy the fluxon's coherency, and, therefore, the observation of the resonant tunneling of fluxons is, in principle, possible.

VI. CONCLUSIONS

In this paper we studied the effect of internal degrees of freedom on tunneling of fluxons through pointlike microshorts. We derived the effective coupling Hamiltonian using the IST technique. Then we investigated the problem using a perturbation scheme and found that at the energies lying deep enough below the barrier's top the tunneling probability is actually enhanced. We interpret these results by introducing a correction to the effective potential which an impurity exerts on a fluxon. This correction may be obtained within the WKB approximation as a static plasmonic potential (analogous to the static "image" potential in the STM). The suppression of the tunneling near the top is due to dynamic corrections,²⁴ which become important when the static correction vanishes.

Our results differ from the "Lorentz expansion" picture proposed in Ref. 4, since the soliton feels a narrower potential barrier than its spatial form implies. We think that the Lorentz expansion is valid for potential barriers which are much wider than a soliton. In the opposite situation (like our) the relaxation of the internal degrees of freedom makes the soliton effectively narrower.

Finally, we have considered the possibility of resonant tunneling of solitons through double impurity barriers. For the case of a few levels in the well, the only effect of plas-

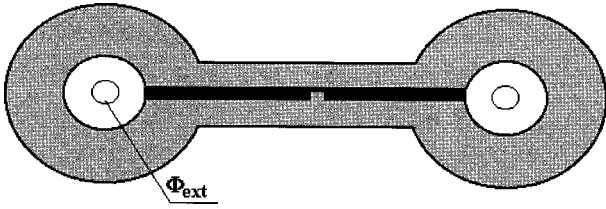


FIG. 4. Experimental setup for fluxons' scattering. The gray area corresponds to a superconductor. The black line is an insulating layer (a long Josephson junction).

mons is the polaron shift of the levels.

The experimental observation of the macroscopic quantum tunneling (MQT) of fluxons may be based on the same idea as the experiment by Voss and Webb.^{26,7} Applying an external current on a circular long Josephson junction with a microshort, one creates a potential well on one side of the microshort. The fluxon will be trapped by the well. When the external current increases the well becomes shallower and, eventually, disappears. Therefore one can measure the average value of the current at which the fluxon escapes from the well. If this value is smaller than the classical escape one, and the temperature is small enough to cause the thermal activation escape, the MQT of fluxons should be observed.^{26,7}

One can also think of measuring the dc V - I characteristic of a very long circular Josephson junction with a microshort. By very long we mean that in between the tunneling events the fluxon moves with the steady-state velocity given by the balance between the driving force (current) and the dissipation.¹¹ Every backward scattering event creates the time delay and, thus, decreases the fluxon's mean velocity (the voltage). For the steady-state kinetic energy larger than the barrier's top energy, some finite voltage should be observed. In the opposite case the voltage is classically zero. Observing a smearing of this step in the I - V curve will serve as evidence of the MQT of fluxons.

Finally, we propose a setup for real scattering experiments with fluxons. Take two thick superconducting rings connected by a long Josephson junction with impurities (See Fig. 4). Insert the Aharonov-Bohm solenoids into the rings. Then, applying an external magnetic flux in one of the solenoids, one creates the screening superconducting current in the corresponding ring, so that the total flux is zero. After some critical value of the external flux, a fluxon will be shut into the junction. If the fluxon tunnels through the impurity, it will be inductively observed in the second ring by the solenoid. This approach can be used to measure both single barrier tunneling as well as resonant tunneling.

ACKNOWLEDGMENTS

The authors thank Y. Aharonov, A. Casher, M. Azbel, R. Mints, V. Fleurov, A. Ustinov, Z. Hermon, G. Guttman F. Guinea, D. Khmel'nitsky, S. Nussinov, and M. Karliner for very fruitful discussions. We thank Alexander van Oudenaarden for informing us about Refs. 27 and 28. This work was partially supported by a Grant from the office of the Vice President for research of Tel-Aviv University.

APPENDIX A: EFFECTIVE HAMILTONIAN DERIVATION

The derivation is based on the fact that one can represent the total Hamiltonian of our system as a sum of the pure sine-Gordon Hamiltonian and impurities' terms:

$$H = H_{SG} + \sum_n \frac{\epsilon_n}{\beta^2} [1 - \cos\Theta(a_n)]. \quad (\text{A1})$$

The sine-Gordon Hamiltonian may be expressed, by means of the IST technique, in terms of new canonical variables, in which the Hamiltonian is decoupled.⁹ Thus our aim is to transform the impurities' terms using the same variables. The essence of the IST is in a mapping of the original sine-Gordon problem into an auxiliary scattering problem, where the field $\Theta(x)$ plays the role of a generalized scattering potential. The wave functions of the auxiliary problem are called the Jost functions and in this particular case they are two-component spinors, $\Psi(x) \equiv \begin{pmatrix} \Psi^{(1)}(x) \\ \Psi^{(2)}(x) \end{pmatrix}$. The scattering data of this auxiliary problem (the forward and backward scattering amplitudes at different values of the spectral parameter) become the new dynamical variables of the system.

We use the equations of the inverse scattering transform as they appear in Ref. 9. The two basic equations determining the relation between the Jost functions and the scattering data are

$$\begin{aligned} \tilde{\Psi}(\lambda, x) e^{i/2i(\lambda - 1/4\lambda)x} &= \begin{pmatrix} 0 \\ 1 \end{pmatrix} + \sum_{n=1}^N \frac{c_n \Psi(\lambda_n, x) e^{i/2(\lambda_n - 1/4\lambda_n)x}}{\lambda - \lambda_n} \\ &+ \frac{1}{2\pi i} \int \frac{r(\mu) \Psi(\mu, x) e^{i/2(\mu - 1/4\mu)x}}{\mu - \lambda + i0} d\mu, \end{aligned} \quad (\text{A2})$$

$$\begin{aligned} \tilde{\Psi}(\lambda_m, x) e^{i/2(\lambda_m^* - 1/4\lambda_m^*)x} &= \begin{pmatrix} 0 \\ 1 \end{pmatrix} + \sum_{n=1}^N \frac{c_n \Psi(\lambda_n, x) e^{i/2(\lambda_n - 1/4\lambda_n)x}}{\lambda_m^* - \lambda_n} \\ &- \frac{1}{2\pi i} \int \frac{r(\mu) \Psi(\mu, x) e^{i/2(\mu - 1/4\mu)x}}{\mu - \lambda_m^*} d\mu, \end{aligned} \quad (\text{A3})$$

where $\tilde{\Psi} \equiv \begin{pmatrix} -\Psi^{(2)*} \\ \Psi^{(1)*} \end{pmatrix}$.

The equation for the backward relation of $\Theta(x)$ in terms of the Jost functions is

$$\begin{aligned} \cos \frac{\theta(x)}{2} &= (-1)^{\Theta(+\infty)/2\pi} \left[1 - \sum_{n=1}^N \frac{c_n}{\lambda_n} \Psi^{(2)} \right. \\ &\times (\lambda_n, x) e^{i/2(\lambda_n - 1/4\lambda_n)x} - \int \frac{r(\mu)}{\mu} \Psi^{(2)} \\ &\left. \times (\mu, x) e^{i/2(\mu - 1/4\mu)x} d\mu \right]. \end{aligned} \quad (\text{A4})$$

In Eqs. (A2)–(A4), the scattering data representing the solitons and the breathers are the c numbers c_n and λ_n ,

while the continuous spectrum scattering data, $r(\mu)$ pertain to the plasmons. Here we consider the situation of one soliton interacting with plasmons. Thus we rewrite Eqs. (A2)–(A4) keeping only a single term in the sums (with the solitonic scattering data which we denote as c_s and λ_s) and the plasmonic (integral) terms. The scattering data c_s , λ_s , and $r(\mu)$ are described by the following formula:

$$\lambda_s = i\eta, \quad \text{Im}(\eta) = 0, \quad (\text{A5})$$

$$r(\mu) = \frac{b(\mu)}{a(\mu)}, \quad (\text{A6})$$

$$\begin{aligned} a(\mu) &= \frac{\mu - \lambda_s}{\mu - \lambda_s^*} \exp\left(\frac{1}{2\pi i} \int d\lambda \frac{\ln(1 - |b(\lambda)|^2)}{\mu - \lambda + i0}\right) \\ &= \frac{\mu - \lambda_s}{\mu - \lambda_s^*} + O(|b^2(\mu)|), \end{aligned} \quad (\text{A7})$$

$$c_s = \frac{b_s}{a'(\lambda_s)} = -2\eta|b_s| + O(|b^2(\mu)|). \quad (\text{A8})$$

The functions $a(\mu)$ and $b(\mu)$ are the elements of the transition (monodromy) matrix (see Ref. 9). Since $b(\mu)$ is proportional to β (see Ref. 9 and below in this section), we neglect all the terms containing $|b(\mu)|$ in the power higher than first.

We solve Eqs. (A2) and (A3) perturbatively in $|b(\mu)|$: $\Psi = \Psi_0 + \Psi_1 + \dots$. In the zeroth order (a pure soliton), we obtain

$$\Psi_0^{(1)}(\lambda_s, x) = \frac{e^{k_s x/2}}{|b_s|^2 e^{-k_s x} + e^{k_s x}}, \quad (\text{A9})$$

$$\Psi_0^{(2)}(\lambda_s, x) = -\frac{i|b_s|e^{-k_s x/2}}{|b_s|^2 e^{-k_s x} + e^{k_s x}}, \quad (\text{A10})$$

$$\Psi_0^{(1)}(\mu, x) = e^{(i/2)k(\mu)x} - \frac{2\eta i|b_s|^2 e^{-[2k_s - ik(\mu)/2]x}}{(\mu + i\eta)(|b_s|^2 e^{-k_s x} + e^{k_s x})}, \quad (\text{A11})$$

$$\Psi_0^{(2)}(\mu, x) = \frac{2\eta|b_s|e^{[ik(\mu)/2]x}}{(\mu + i\eta)(|b_s|^2 e^{-k_s x} + e^{k_s x})}. \quad (\text{A12})$$

Here we introduced the notation: $k(\mu) \equiv (\mu - 1/4\mu)$ and $k_s \equiv k(\lambda_s)/i$.

Looking at Eq. (A4), we see that, to calculate $\cos(\theta/2)$ at the first order in $|b(\mu)|$, we need to know only the expression for $\Psi_1^{(2)}(\lambda_s, x)$ [the integral term of Eq. (A4) contains already one power of $|b(\mu)|$]. Using Eq. (A3) we get

$$\begin{aligned} \Psi_1^{(2)}(\lambda_s, x) &= \frac{1}{e^{k_s x/2} + |b_s|^2 e^{-3k_s x/2}} \left(\frac{|b_s|e^{-k_s x}}{2\pi} \right. \\ &\quad \times \int d\mu \frac{b(\mu)e^{i/2k(\mu)x}}{\mu - i\eta} \Psi_0^{(2)}(\mu, x) - \frac{1}{2\pi i} \\ &\quad \left. \times \int d\mu \frac{b^*(\mu)e^{-(i/2)k(\mu)x}}{\mu + i\eta} \Psi_0^{(1)*}(\mu, x) \right). \end{aligned} \quad (\text{A13})$$

We now substitute Eqs. (A9)–(A13) into Eq. (A4) and we obtain

$$\begin{aligned} \cos \frac{\theta(x)}{2} &= \frac{z^2 - 1}{z^2 + 1} + \frac{2z(z^2 - 1)}{(z^2 + 1)^2} \frac{i\eta}{\pi} \int d\mu \frac{f(\mu)}{\mu^2 + \eta^2} \\ &\quad - \frac{z}{z^2 + 1} \frac{1}{\pi} \int d\mu \frac{f(\mu)}{\mu} \frac{\mu^2 - \eta^2}{\mu^2 + \eta^2}, \end{aligned} \quad (\text{A14})$$

where $z \equiv |b_s|e^{-k_s x}$ and $f(\mu) \equiv b(\mu)e^{ik(\mu)x}$.

Using the identity $(1 - \cos \theta) = 2 - 2 \cos^2 \theta/2$ we obtain from Eq. (A14) the impurity contribution to the Hamiltonian (A1). Finally, we change the integration variable μ into $k(\mu)$ and transform all the expressions to the new dynamical variables:

$$P = -\frac{8}{\beta^2} \left(\eta - \frac{1}{4\eta} \right), \quad (\text{A15})$$

$$X = \frac{\ln|b_s|}{(\eta + 1/4\eta)} \quad (\text{A16})$$

$$d_k = \sqrt{p_k} e^{iq_k}, \quad d_k^* = \sqrt{p_k} e^{-iq_k}, \quad (\text{A17})$$

where

$$p_k = \frac{4}{\beta^2 \pi \omega_k} |b(k)|^2,$$

$$q_k = \arg(b(k)),$$

$$b(k) \equiv b(\mu(k)),$$

$$\omega_k \equiv \sqrt{1 + k^2}. \quad (\text{A18})$$

In the nonrelativistic approximation ($\eta + 1/4\eta \approx 1$) we obtain the Hamiltonian (7).

APPENDIX B: PERTURBATION SCHEME AND SCATTERING MATRIX ELEMENTS

First we develop a perturbation scheme which treats fluxons' tunneling across potential barrier V_0 in zeroth approximation. The S matrix emerging in such a scheme is slightly unusual, since it connects not the free fluxon and free plasmon states, but the fluxon states distorted by the potential V_0 and the free plasmon states. Let us denote by $\Psi_{E,+}$ ($\Psi_{E,-}$) the scattering fluxon state with the energy E , corresponding to an incident wave arriving from the left (right). We normalize these states such that

$$\langle \Psi_{E_1,d} | \Psi_{E_2,f} \rangle = \delta(E_1 - E_2) \delta_{d,f}. \quad (\text{B1})$$

Then the S matrix is determined by the following set of the matrix elements:

$$\langle n_{k_1}, n_{k_2}, \dots, \Psi_{E_1,+} | S | n_{q_1}, n_{q_2}, \dots, \Psi_{E_2,\pm} \rangle, \quad (\text{B2})$$

where n_k and n_q are the plasmon numbers in the ‘‘in’’ and ‘‘out’’ states, respectively. The only δ function which should appear in Eq. (B2) is one accounting for conservation of energy. The total momentum is not conserved since scattering is on a stiff potential barrier. The wave functions $\Psi_{E,+}$

and $\Psi_{E,-}$ are known exactly for the one-barrier case,²² so we can construct an exact fluxon Green function $G_0(X_1, X_2, E)$, which will appear in the perturbation theory expansion as a fluxon's propagator.

In this paper we are mostly interested in the elastic processes at zero temperature, i.e., the processes with zero energy transfer to the plasmons. Thus, we should calculate only two matrix elements of S . These are

$$A(E) = \langle \Psi_{E,+} | S - 1 | \Psi_{E,+} \rangle, \quad (\text{B3})$$

and

$$B(E) = \langle \Psi_{E,+} | S | \Psi_{E,-} \rangle. \quad (\text{B4})$$

To construct the new elastic-scattering state, one should add to the unperturbed state $\Psi_{E,+}$ the outgoing waves corresponding to $\Psi_{E,+}$ with the amplitude $A(E)$ and the outgoing waves corresponding to $\Psi_{E,-}$ with the amplitude $B(E)$. Then, if $t_0(E)$ and $r_0(E)$ are the transmission and reflection amplitudes without fluxon-plasmons coupling, the renormalized elastic-scattering amplitudes are given by

$$t(E) = (1 + A)t_0 - B r_0^* \frac{t_0}{t_0^*}, \quad (\text{B5})$$

$$r(E) = (1 + A)r_0 + B t_0. \quad (\text{B6})$$

We evaluate the matrix elements (B3) and (B4) using the diagrammatic technique. First, we calculate the zeroth-order (free) propagators. The plasmon propagator is the standard one:

$$D(k, \omega) \equiv -i \int dt e^{i\omega t} \langle T(d_k(t) d_k^\dagger(0)) \rangle = \frac{1}{\omega - \omega_k + i\delta}. \quad (\text{B7})$$

We construct the fluxon propagator, using the exact wave functions: $\Psi_{E,+}$ and $\Psi_{E,-}$, given in Ref. 22:

$$\Psi_{E,\pm} = \frac{1}{\sqrt{2\pi v}} t(s, k) e^{\pm ikx} F\left(s + 1, -s, 1 - ik, \frac{1 \pm \tanh x}{2}\right), \quad (\text{B8})$$

where v is the fluxon's classical velocity $v = k\beta^2/8$ and $F(\dots)$ denotes the hypergeometric function.

$$t(s, k) = \frac{\Gamma(-s - ik)\Gamma(1 + s - ik)}{\Gamma(1 - ik)\Gamma(-ik)}, \quad (\text{B9})$$

is a transmission amplitude for a soliton having the wave number k , $\Gamma(\cdot)$ stands for the gamma function, and

$$s = -\frac{1}{2} + \frac{i}{2} \sqrt{\frac{128\epsilon}{\beta^4} - 1}. \quad (\text{B10})$$

Then the fluxon propagator is given by

$$G_0(x_1, x_2, \omega) = \sum_{E_s, d=\pm} \frac{\Psi_{E_s, d}(x_1) \Psi_{E_s, d}(x_2)}{\omega - E_s + i\delta}. \quad (\text{B11})$$

Finally, the matrix elements A and B are

$$A(E) = -\frac{\epsilon^2 i}{8\beta^2} \sum_{j=1,2} \sum_{E_s, d=\pm} \langle \Psi_{E,+} | V_j | \Psi_{E_s, d} \rangle \times \langle \Psi_{E_s, d} | V_j | \Psi_{E,+} \rangle I_j(E - E_s), \quad (\text{B12})$$

$$B(E) = -\frac{\epsilon^2 i}{8\beta^2} \sum_{j=1,2} \sum_{E_s, d=\pm} \langle \Psi_{E,+} | V_j | \Psi_{E_s, d} \rangle \times \langle \Psi_{E_s, d} | V_j | \Psi_{E,-} \rangle I_j(E - E_s), \quad (\text{B13})$$

where

$$I_1(E - E_s) = \int dk \frac{1}{\omega_k^3 (E - E_s - \omega_k + i\delta)}, \quad (\text{B14})$$

$$I_2(E - E_s) = \int dk \frac{k^2}{\omega_k^3 (E - E_s - \omega_k + i\delta)}. \quad (\text{B15})$$

The integrals (B14) and (B15) can be calculated exactly. So, the only problem is to evaluate the matrix elements in Eqs. (B12) and (B13). One can see that the expression for the real part of $A(E)$ includes only the imaginary parts of $I_j(E - E_s)$, which are zero at $E - E_s < 1$ (the plasmon gap). For $E - E_s > 1$, the matrix elements are exponentially small, so $\text{Re}(A)$ is exponentially small too.

To approximate the expression for the $\text{Re}(B)$ we assume that the absolute values of the matrix elements in Eq. (B13) decrease quickly with the increase of $|E - E_s|$. Then we expand the functions I_1 and I_2 up to the first degree of $(E - E_s)$ around the point $E - E_s = 0$, and we insert the expressions $(E - E_s)$ into the matrix elements using the standard way:

$$(E - E_s) \langle \Psi_{E,+} | V_j | \Psi_{E_s, d} \rangle = \langle \Psi_{E,+} | [H_0, V_j] | \Psi_{E_s, d} \rangle, \quad (\text{B16})$$

where H_0 is given by Eq. (13) (without the plasmon term). Using the completeness relation we, finally, arrive at the first Born-approximation-like expression

$$\text{Re}(B(E)) = 2\pi \langle \Psi_{E,+} | \Delta V_{\text{Born}} | \Psi_{E,-} \rangle, \quad (\text{B17})$$

where ΔV_{Born} is given by Eq. (17).

¹P. C. A. Stamp, Phys. Rev. Lett. **66**, 2802 (1991).

²P. Ao and D. J. Thouless, Phys. Rev. Lett. **72**, 132 (1994).

³A. O. Caldeira and A. J. Leggett, Ann. Phys. (N.Y.) **149**, 374 (1983).

⁴F. Guinea, R. Peierls, and J. R. Schrieffer, Phys. Scr. **33**, 282 (1986).

⁵A. I. Larkin and P. A. Lee, Phys. Rev. B **17**, 1596 (1978).

⁶Mesoscopic Phenomena in Solids, edited by B. L. Altshuler, P. A. Lee, and R. A. Webb (North-Holland, Amsterdam, 1991).

⁷T. Kato and M. Imada, J. Phys. Soc. Jpn. **65**, 2963 (1996).

⁸G. Schön and A. D. Zaikin, Phys. Rep. **198**, 237 (1990).

⁹S. Novikov, S. V. Manakov, L. P. Pitaevskii, and V. E. Zharov, *The Inverse Scattering Method* (Consultants Bureau, New York, 1984), Chap. 1, Part 11.

- ¹⁰Z. Hermon, A. Stern, and E. Ben-Jacob, Phys. Rev. B **49**, 9757 (1994).
- ¹¹D. W. McLaughlin and A. C. Scott, Phys. Rev. A **18**, 1652 (1978).
- ¹²D. J. Bergman, E. Ben-Jacob, Y. Imry, and K. Maki, Phys. Rev. A **27**, 3345 (1983).
- ¹³R. Rajaraman, *Solitons and Instantons* (North-Holland, Amsterdam, 1982).
- ¹⁴Z. Hermon, A. Shnirman, and E. Ben-Jacob, Phys. Rev. Lett. **74**, 4915 (1995).
- ¹⁵R. Dashen, B. Hasslacher, and A. Neveu, Phys. Rev. D **11**, 3424 (1975).
- ¹⁶Z. Hermon, E. Ben-Jacob, and G. Schön, Phys. Rev. B **54**, 1234 (1996).
- ¹⁷D. J. Kaup, SIAM (Soc. Ind. Appl. Math.) J. Appl. Math. **31**, 121 (1976).
- ¹⁸V. I. Karpman and E. M. Maslov, Phys. Lett. **60A**, 307 (1977).
- ¹⁹Yu. S. Kivshar and B. A. Malomed, Rev. Mod. Phys. **61**, 763 (1989).
- ²⁰A. Widom, Phys. Rev. B **21**, 5166 (1980).
- ²¹G. D. Mahan, *Many Particle Physics* (Plenum, New York, 1981).
- ²²L. D. Landau and E. M. Lifshits, *Quantum Mechanics, Nonrelativistic Theory* (Pergamon, Oxford, 1965), Part 25.
- ²³M. Buttiker and R. Landauer, Phys. Rev. Lett. **49**, 1739 (1982).
- ²⁴B. N. J. Persson and A. Baratoff, Phys. Rev. B **38**, 9616 (1988).
- ²⁵L. I. Glazman and R. I. Shekhter, Sov. Phys. JETP **67**, 163 (1988).
- ²⁶R. F. Voss and R. A. Webb, Phys. Rev. Lett. **47**, 265 (1981).
- ²⁷Alexander van Oudenaarden and J. E. Mooij, Phys. Rev. Lett. **76**, 4947 (1996).
- ²⁸Mathys Robbens and Alexander van Oudenaarden (private communication).